

Electronic state calculations of Si quantum dots: Oxidation effects

Masahiko Nishida*

Physics Department, Kanazawa Institute of Technology, Nonoichi-machi, Ishikawa 921-8501, Japan
(Received 18 September 2003; revised manuscript received 17 February 2004; published 29 April 2004)

Electronic states for the configuration of a Si dihydride backbonded to oxygen on the H-covered surface of spherical $\text{Si}_{35}\text{H}_{36}$ quantum dots (QDs) are calculated self-consistently using the extended Hückel-type nonorthogonal tight-binding method. The proposed backbond oxidation accounts for oxidation-induced redshifts in luminescence-peak energy observed in porous Si. It is found that optical transitions between the band edges in the Si QD backbonded to oxygen are dipole allowed as in the H-covered case. A comparison is made with a calculation for the double-bonded oxygen configuration.

DOI: 10.1103/PhysRevB.69.165324

PACS number(s): 73.22.Dj, 73.20.At, 78.67.Bf

I. INTRODUCTION

It is well established that Si nanocrystals in porous Si prepared electrochemically in HF-based solutions can emit efficient visible photoluminescence (PL) at room temperature, and the surface is passivated by hydrogen.¹ However, oxidation takes place easily on the H-covered surface of porous Si, and thus the light-emitting process is extremely sensitive to oxygen.^{1,2} A typical effect of oxidation on the PL spectra is an observed redshift in the PL-peak energy. A double-bonded oxygen model has been proposed for explaining the phenomenon.² The configuration of double-bonded oxygen in the model significantly affects the band-edge states and accounts for the observed redshifts in the band gap of Si nanocrystals studied.²⁻⁵ However, proposed optical transitions between a *p*-like electron state localized on the Si atom in the Si=O bond and a *p*-like hole state localized on the oxygen atom are not dipole allowed.²⁻⁴ In this oxygen configuration, therefore, it would be difficult to have band-edge optical transitions as strong as those in H-covered Si nanocrystals.

In this paper, an alternative oxidation model, in which oxygen is put at a backbond site between a surface Si hydride and its nearest-neighbor Si atom on H-covered Si nanocrystals, is proposed for explaining the redshifts in the band gap of Si nanocrystals. Experimentally, many Fourier transform infrared (FTIR) studies of H-covered porous Si exposed to oxygen have observed the blueshifting of the Si—H stretching vibration modes as oxidation progresses (frequency shifting to the blue compared to the parent Si—H stretching modes) in addition to the observation of the Si—O—Si modes, and have indicated the formation of surface Si hydride species backbonded to oxygen atoms by oxygen incorporation into the Si—Si backbonds on the H-covered surface.⁶ Other FTIR measurements have also revealed that, in anodically oxidized porous Si, the oxidation occurs at the Si—Si backbonds of the surface Si atoms, while the hydrogen coverage on the surface is preserved.⁷ So far, no FTIR signal of a vibration mode associated directly with the formation of the Si=O bonds on the surface of porous Si has been reported in the literature.^{6,7} Hence, we can say that the oxidation of H-covered porous Si, at its initial stage at least, results in the formation of Si hydrides

backbonded to oxygen on the surface with the amount of hydrogen preserved.

Here, a Si nanocrystal is simulated by a spherical $\text{Si}_{35}\text{H}_{36}$ quantum dot (QD) terminated by hydrogen, and electronic state calculations are done using the extended Hückel-type nonorthogonal tight-binding (EHNTB) method.⁸ We pay attention to the electronic structure of the highest occupied molecular orbital (HOMO) and the lowest unoccupied molecular orbital (LUMO) states. In this paper the HOMO and LUMO are referred to as the valence-band (VB) and conduction-band (CB) edges, respectively, in terms of solid-state physics. The HOMO-LUMO gap is referred to as the band gap. Not only the calculated band gaps, but also the characteristics of the band-edge states and optical transitions between the band edges in the oxidized $\text{Si}_{35}\text{H}_{36}$ QD, are also described in comparison with those in the unoxidized (H-terminated) QD. It is shown that the backbond oxidation of the H-covered Si QD explains the experimentally observed redshifts in the band gap, and that optical transitions between the band edges in the oxidized QD are dipole allowed as in the H-covered case.

II. MODEL AND CALCULATIONS

The $\text{Si}_{35}\text{H}_{36}$ QD is constructed by starting with a central Si atom and sequentially adding its nearest-neighbor shells of Si atoms up to the fourth one. Figure 1(a) schematically shows the atom configuration of the $\text{Si}_{35}\text{H}_{36}$ QD as viewed along one of six $\langle 100 \rangle$ orientations. The dangling bonds occurring on the QD surface are passivated by hydrogen atoms [not shown in Fig. 1(a) for clarity] along the tetrahedral bond directions (the lattice constant *a* for Si is 5.43 Å and the Si—H bond length is taken as 1.48 Å). We simulate a surface Si hydride backbonded to oxygen by putting an O atom at a backbond site between a Si dihydride at the top of the $\text{Si}_{35}\text{H}_{36}$ QD and its nearest-neighbor Si atom in the second monolayer along the [001] direction, as shown in Fig. 1(b). Hereafter this oxidized QD is referred to as the $\text{Si}_{35}\text{H}_{36}\text{O}$ QD. The Si—O—Si angle β is taken as 151°. This value of β is the mean value of the expected Si—O—Si bond-angle distribution in vitreous silica.⁹ A recent first-principles nuclear magnetic resonance analysis for the Si—O—Si bond-angle distribution in vitreous SiO_2 has shown that the Si—O—Si angle varies from 120° to 180° around a mean

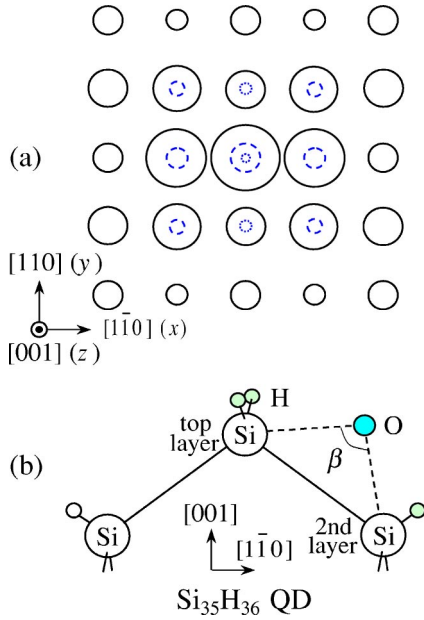


FIG. 1. (Color online) (a) Plan of the Si-atom configuration of the $\text{Si}_{35}\text{H}_{36}$ quantum dot as viewed along the $[001]$ direction. The size of a circle indicates the proximity of that atom to the (001) surface at the top of the QD. The dotted circles show the Si atoms lying exactly below the ones denoted by the solid circles. The hydrogen atoms saturating dangling bonds are not shown for simplicity. (b) Schematic configuration of the QD backbonded to oxygen, denoting a Si dihydride and two Si monohydrides. The angle β is the Si—O—Si angle.

value and the mean is 151° .⁹ The length of the Si—O bond is taken as 1.64 \AA . Then the backbond to which oxygen attaches is elongated to 3.18 \AA . The position of the Si dihydride at the top of the QD after oxidation is determined so as to preserve the length of the remaining Si—Si backbond (2.35 \AA). The other parameters are kept the same as those in the unoxidized case. It should be noted that the proposed backbond oxidation does not need advance hydrogen desorption and thus the number of H atoms passivating the Si dots is preserved on the occasion of the oxidation, in contrast to the previously reported oxidation models (double-bonded oxygen model²⁻⁵ and bridging oxygen model⁴) in which two H atoms on the surface are replaced with one O atom. The preservation of the number of H atoms in a Si dot is in agreement with the experimental observations in which the H coverage on the surface of porous Si is preserved.⁷ For comparison, the EHNTB calculations for the double-bonded oxygen configuration are also performed by putting an O atom replacing the two H atoms on the top-layer Si atom of the Si_{35} QD (referred to as the $\text{Si}_{35}\text{H}_{34}\text{O}$ QD hereafter).

The EHNTB method explicitly calculates all distant-neighbor overlap and energy integrals between atomic orbitals (simulated by Slater-type atomic orbitals) in a QD up to the sixth-nearest neighbors, in contrast to conventional tight-binding methods in which overlap integrals between atomic orbitals are neglected. The EHNTB parameters associated with Si, H, and O have been determined so as to accurately reproduce the Si band structure, and H- and O-related surface

states on the Si surface, respectively. The parameters between H and O have been determined so as to reproduce the molecular-orbital (MO) energy levels of the free H_2O molecule. Special care has been given to the quantitatively precise reproduction of the CB as well as the VB across the Brillouin zone by the EHNTB method, which enables one to study the optical properties of Si nanostructures. See Ref. 8 for more details. Here, in order to include charge transfer effects due to oxidation, we incorporate self-consistency in the EHNTB calculations according to Ref. 10. More specifically, we introduce a charge-dependent potential I_{ap} given by $I_{ap} = I_\alpha + Q\gamma_{\alpha\alpha}$ for an orbital α in an atom, where I_α is the ionization potential in the neutral atom, Q a net charge of the atom, and $\gamma_{\alpha\alpha}$ a one-center electron-repulsion integral given by $\gamma_{\alpha\alpha} = I_\alpha - A_\alpha$ for $Q < 0$ and $\gamma_{\alpha\alpha} = I'_\alpha - I_\alpha$ for $Q > 0$. Here A_α and I'_α are the electron affinity and second ionization potential for the orbital α , respectively. The EHNTB calculations are carried out iteratively until self-consistency in charge is obtained between a QD and oxygen. The charge is calculated using a Mulliken charge-population analysis of MO energies and coefficients.¹¹

For the purpose of analyzing the character of the electronic states at the CB and VB, the orbital density of states is calculated from the following equation (1) for an orbital α at energy ε , by giving each energy level a Gaussian broadening with a half width (ω) of 0.05 eV :

$$D_\alpha(\varepsilon) = \frac{2}{\sqrt{\pi}\omega} \sum_n C_{an} \sum_\beta C_{\beta n} S_{\alpha\beta}^n \exp\left(-\frac{(\varepsilon - \varepsilon_n)^2}{\omega^2}\right), \quad (1)$$

where ε_n is the n th eigenvalue (MO energy) of the system, the C_{an} 's the MO coefficients, and $S_{\alpha\beta}^n$ the overlap integral between the α th and β th orbitals in the n th MO. We obtain the local density of states (LDOS) for silicon, hydrogen, and oxygen separately by summing the orbital density of states calculated for each orbital over the Si, H, and O atoms contained in the QD studied.

The oscillator strength f (unitless) and the radiative lifetime τ for dipole-allowed optical transitions are calculated by the following equations:¹²

$$f = \frac{2}{3mE_g} \langle \psi_c | \mathbf{p} | \psi_v \rangle^2, \quad (2)$$

$$\frac{1}{\tau} = \frac{ne^2 E_g^2 f}{2\pi \varepsilon_0 m c^3 \hbar^2}, \quad (3)$$

where E_g is the band gap between the CB and VB edges, and $\langle \psi_c | \mathbf{p} | \psi_v \rangle$ the momentum matrix element between the band edges for unpolarized light, m the electron mass, n the refractive index ($n = 2.6$), e the electronic charge, ε_0 the electric permittivity of free space, and c the speed of light. In the EHNTB method, the momentum matrix elements $\langle \psi_c | \mathbf{p} | \psi_v \rangle$ are calculated directly from a linear combination of momentum matrix elements between atomic orbitals simulated by Slater-type atomic orbitals.⁸

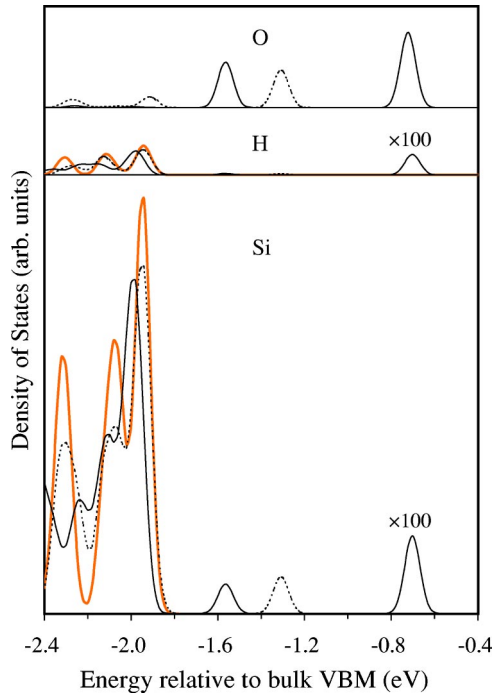


FIG. 2. (Color online) Calculated local densities of states in the valence band for Si, hydrogen, and oxygen in the $\text{Si}_{35}\text{H}_{36}\text{O}$ QD backbonded to oxygen (solid lines) and the $\text{Si}_{35}\text{H}_{34}\text{O}$ QD double bonded to oxygen (dotted lines), in comparison with those for the unoxidized QD (thick lines). The energy is relative to the bulk valence band maximum.

III. RESULTS AND DISCUSSION

Figure 2 presents the calculated LDOSs in the VB for Si, hydrogen, and oxygen in the $\text{Si}_{35}\text{H}_{36}\text{O}$ QD (solid lines), in comparison with those for the $\text{Si}_{35}\text{H}_{34}\text{O}$ QD (dotted lines) and for the unoxidized QD (thick lines). The energy is relative to the bulk VBM (VB maximum). As seen in the figure, the electronic states near the VB edge are largely changed by oxidation as compared to the triply degenerate VB edge (at

~ -2 eV) for the unoxidized case. It is found that two new states (at ~ -1.55 and -0.7 eV) and one new state (at ~ -1.3 eV) occur in the $\text{Si}_{35}\text{H}_{36}\text{O}$ and $\text{Si}_{35}\text{H}_{34}\text{O}$ QDs, respectively. It is noted that the VB edge is more upshifted by the backbond oxidation than by the double-bonded oxidation, contributing to a narrowing of the band gap. We find that there is a large amount of O contribution near the VB edge in both Si QDs. The large O contribution to the VB edge arises from a bonding interaction between the O and Si atoms, as expected. In the $\text{Si}_{35}\text{H}_{36}\text{O}$ QD backbonded to oxygen, the lower new state at ~ -1.55 eV is composed mainly of the p -like O and Si states in the Si—O—Si bond. In particular, the energy upshift of the VB edge (the upper new state at ~ -0.7 eV) in the $\text{Si}_{35}\text{H}_{36}$ QD is caused by a large electron transfer from the QD to oxygen ($\sim 0.48e$), thereby leading to the formation of a π bond (along the $[110]$ direction) between the O and Si atoms in the Si—O—Si bond. The Si contribution to the VB edge is found to be small but still significant. On the other hand, the VB-edge state of the $\text{Si}_{35}\text{H}_{34}$ QD double-bonded to oxygen is composed mostly of the O p_x orbital state (along the $[1\bar{1}0]$ direction) with some amount of Si states. In this case the calculated amount of electrons transferred from $\text{Si}_{35}\text{H}_{34}$ QD to oxygen is $\sim 0.39e$.

In order to clarify the character of the band-edge states in more detail, we show in Fig. 3 the enlarged LDOS for Si at the VB edge of the (a) $\text{Si}_{35}\text{H}_{36}\text{O}$ QD (solid lines), in comparison with that of the (b) $\text{Si}_{35}\text{H}_{34}\text{O}$ (dotted lines) QD. The LDOSs for the top to ninth monolayers of Si along the $[001]$ direction are shown, respectively, in the top to bottom curves. As expected, the Si atoms near the O atom contribute to the VB-edge states in both $\text{Si}_{35}\text{H}_{36}\text{O}$ and $\text{Si}_{35}\text{H}_{34}\text{O}$ QDs, which extend up to the fifth Si monolayer along the $[001]$ direction. It should be noted that, as compared to that of the third-layer Si atoms, the contribution of the top-layer Si atom is negligible at the VB edge of the $\text{Si}_{35}\text{H}_{36}\text{O}$ QD backbonded to oxygen. Thus, the character of the O-induced VB-edge state in the $\text{Si}_{35}\text{H}_{36}\text{O}$ QD reflects the fact that the top-layer Si atom is significantly isolated from the rest of the QD because

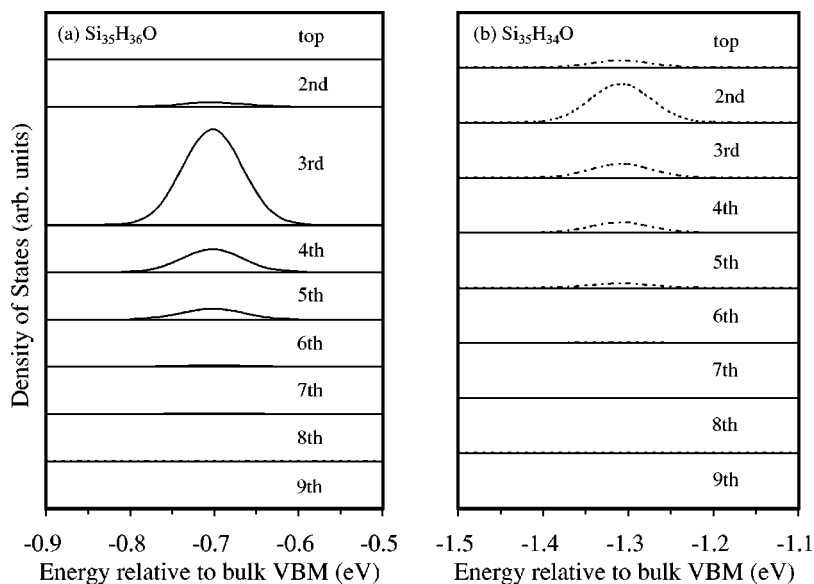


FIG. 3. Enlarged local density of states for Si at the valence-band edge of the (a) $\text{Si}_{35}\text{H}_{36}\text{O}$ QD and (b) $\text{Si}_{35}\text{H}_{34}\text{O}$ QD relative to the bulk VBM. From top to bottom, the curves show, respectively, the LDOSs for the top to ninth monolayers of Si along the $[001]$ direction in the Si_{35} QD.

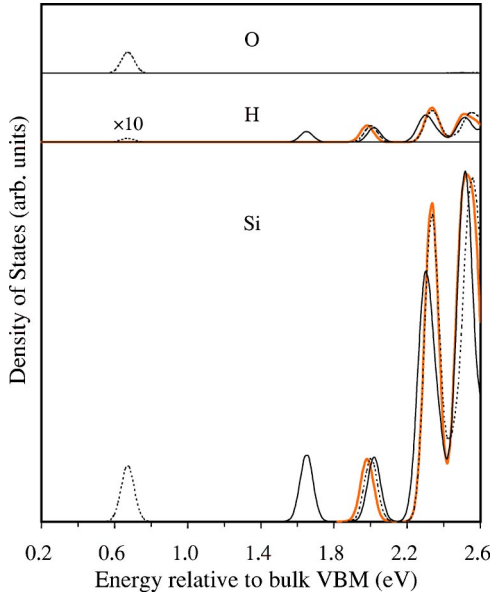


FIG. 4. (Color online) Calculated local densities of states in the conduction band for Si, hydrogen, and oxygen in the $\text{Si}_{35}\text{H}_{36}\text{O}$ QD (solid lines) and the $\text{Si}_{35}\text{H}_{34}\text{O}$ QD (dotted lines), in comparison with those for the unoxidized QD (thick lines).

of the formation of the Si—O—Si bond at the backbond site.

Figure 4 shows the calculated LDOSs in the CB for Si, hydrogen, and oxygen in the $\text{Si}_{35}\text{H}_{36}\text{O}$ QD (solid lines), in comparison with those for the $\text{Si}_{35}\text{H}_{34}\text{O}$ QD (dotted lines) and for the unoxidized QD (thick lines). We can see a drastic change in electronic structure near the CB edge due to oxidation as compared to the electronic structure of the CB edge (at ~ 2 eV) of the unoxidized QD, and the oxidation-induced localized CB-edge state occurs at about 0.7 and 1.65 eV above the VBM in the $\text{Si}_{35}\text{H}_{34}\text{O}$ QD and $\text{Si}_{35}\text{H}_{36}\text{O}$ QD, respectively. The CB-edge state at ~ 0.7 eV in the $\text{Si}_{35}\text{H}_{34}\text{O}$ QD is due to a pure π bond formed between the p_y orbital of the O atom and that of the top-layer Si atom. This is in agreement with the result calculated by Wolkin *et al.*² On the other hand, we find that while oxygen contribution is negligible, there is a significant amount of H contribution to the oxidation-induced CB-edge state of the $\text{Si}_{35}\text{H}_{36}\text{O}$ QD. This H contribution arises mostly from the dihydride on the top-layer Si atom and the monohydrides on the second-layer Si atoms [see Fig. 1(b)].

Figure 5 shows the enlarged LDOSs for Si at the CB edge of the $\text{Si}_{35}\text{H}_{36}\text{O}$ QD (solid lines), in comparison with that of the $\text{Si}_{35}\text{H}_{34}\text{O}$ (dotted lines) QD. As stated above, the top-layer Si atom contributes outstandingly to the CB-edge state in the $\text{Si}_{35}\text{H}_{34}\text{O}$ QD. On the other hand, the Si atoms lying away from as well as near the O atom contribute to the CB-edge state in the $\text{Si}_{35}\text{H}_{36}\text{O}$ QD, which extends up to the fifth Si monolayer along the [001] direction.

Finally, the calculated band gaps, oscillator strengths, and radiative lifetimes for the Si_{35} QDs studied are given in Table I. We find that the calculated band gap can be greatly redshifted when one O atom is incorporated in both QDs, in qualitative agreement with the experimental observations in

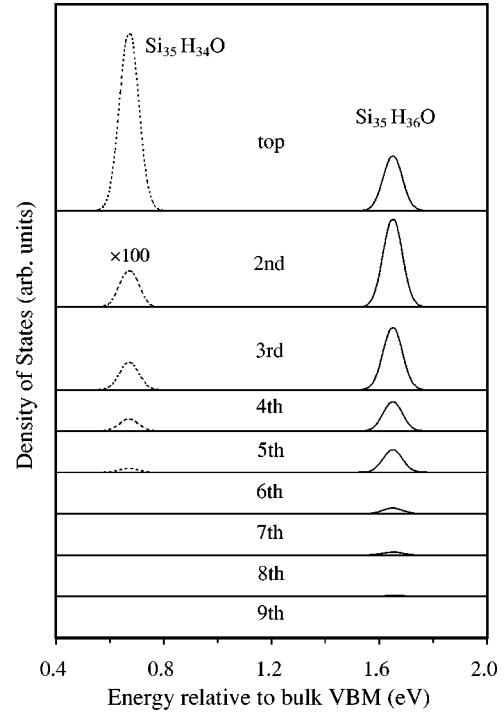


FIG. 5. Enlarged local density of states for Si at the conduction-band edge of the $\text{Si}_{35}\text{H}_{36}\text{O}$ QD (solid lines) and $\text{Si}_{35}\text{H}_{34}\text{O}$ QD (dotted lines). See also the caption of Fig. 3.

porous Si.² However, it is noted that optical transitions between the band edges in the $\text{Si}_{35}\text{H}_{36}$ QD backbonded to oxygen are dipole allowed, in striking contrast to those in the double-bonded oxygen configuration.^{2,3} In fact, in the present study the oscillator strength calculated for the band edges of the $\text{Si}_{35}\text{H}_{34}\text{O}$ QD is found to be very small (1.87×10^{-9}) as shown in Table I. This is because the CB-edge state (at ~ 0.7 eV) of the $\text{Si}_{35}\text{H}_{34}\text{O}$ QD is composed mostly of the p -like states of the O and top-layer Si atoms as stated above. In addition to the double-bonded oxygen configuration, Vasiliev, Chelikowsky, and Martin have studied a configuration in which oxygen forms a Si—O—Si bond bridging two Si atoms on the (111) surface of the Si_{35} QD (a bridging oxygen configuration).⁴ They found that, although the size of the optical gaps is greatly reduced, optical transitions between the band edges in the bridging O configuration are also not dipole allowed, in contrast to the present backbond-oxidation configuration. The calculated radiative lifetimes for the band-edge transitions in the present study

TABLE I. Calculated band gap (E_g), oscillator strength (f) for unpolarized light, and radiative lifetime (τ) in the Si_{35} quantum dots before and after oxidation. The $\text{Si}_{35}\text{H}_{36}\text{O}$ and $\text{Si}_{35}\text{H}_{34}\text{O}$ QDs are the dots backbonded and double bonded to oxygen, respectively.

	$\text{Si}_{35}\text{H}_{36}$	$\text{Si}_{35}\text{H}_{36}\text{O}$	$\text{Si}_{35}\text{H}_{34}\text{O}$
E_g (eV)	3.92	2.35	2.00
f ($\times 10^{-3}$)	0.141	0.985	1.87×10^{-6}
τ (μs)	4.13	1.64	1.10×10^6

are found to be in the microsecond range as shown in Table I, in good agreement with the measurements in porous Si.²

IV. CONCLUSIONS

In summary, electronic states for the configuration of a Si dihydride backbonded to oxygen on the surface of a spheri-

cal Si₃₅H₃₆ QD have been calculated self-consistently using the EHNTB method. A comparison has been made with a calculation for the double-bonded oxygen configuration. It has been shown that the backbond oxidation of the H-covered Si QD causes large redshifts in the band gap, and that an optical transition between the band-edge states is dipole allowed as in the H-covered case, in striking contrast to the case of the double-bonded oxygen configuration.

*Email address: m.nishida@neptune.kanazawa-it.ac.jp

¹A. G. Cullis, L. T. Canham, and P. D. J. Calcott, *J. Appl. Phys.* **82**, 909 (1997).

²M. V. Wolkin, J. Jorne, P. M. Fauchet, G. Allan, and C. Delerue, *Phys. Rev. Lett.* **82**, 197 (1999).

³A. Puzder, A. J. Williamson, J. C. Grossman, and G. Galli, *J. Chem. Phys.* **117**, 6721 (2002).

⁴I. Vasiliev, J. R. Chelikowsky, and R. M. Martin, *Phys. Rev. B* **65**, 121302 (2002).

⁵Y. Dai, S. Han, D. Dai, Y. Zhang, and Y. Qi, *Solid State Commun.* **126**, 103 (2003); M. Luppi and S. Ossicini, *J. Appl. Phys.* **94**, 2130 (2003).

⁶Y. Kato, T. Ito, and A. Hiraki, *Jpn. J. Appl. Phys., Part 2* **27**, L1406 (1988); P. Gupta, A. C. Dillon, A. S. Bracker, and S. M. George, *Surf. Sci.* **245**, 360 (1991); K. H. Li, C. Tsai, and J. C. Cambell, *J. Electron. Mater.* **23**, 409 (1994); Y. Ogata, H. Niki, T. Sakka, and M. Iwasaki, *J. Electrochem. Soc.* **142**, 1595 (1995); P. O'Keeffe, S. Komuro, T. Kato, T. Morikawa, and Y. Aoyagi, *Appl. Phys. Lett.* **66**, 836 (1995); H. Chen, X. Hou, G.

Li, F. Zhang, M. Yu, and X. Wang, *J. Appl. Phys.* **79**, 3282 (1996); D. B. Mamhinney, J. A. Glass, Jr., and J. T. Yates, Jr., *J. Phys. Chem. B* **101**, 1202 (1997).

⁷E. B. Vazsonyi, M. Koos, G. Jalsovszky, and I. Pocsik, *J. Lumin.* **57**, 121 (1993); S. Shih, K. H. Jung, J. Yan, D. L. Kwong, M. Kovar, J. M. White, M. George, and S. Kim, *Appl. Phys. Lett.* **63**, 3306 (1993); M. A. Hory, R. Herino, M. Ligeon, F. Muller, F. Gaspard, L. Mihalcescu, and J. C. Vial, *Thin Solid Films* **255**, 200 (1995).

⁸M. Nishida, *Phys. Rev. B* **58**, 7103 (1998); **59**, 15 789 (1999); **60**, 8902 (1999); *Solid State Commun.* **116**, 655 (2000).

⁹F. Mauri, A. Pasquarello, B. G. Pfrommer, Y. G. Yoon, and S. G. Louie, *Phys. Rev. B* **62**, R4786 (2000).

¹⁰M. Lannoo and J. Bourgoin, in *Point Defects in Semiconductors I*, edited by M. Cardona (Spring-Verlag, New York, 1981), p. 123.

¹¹R. S. Mulliken, *J. Chem. Phys.* **23**, 1933 (1955).

¹²P. K. Basu, *Theory of Optical Processes in Semiconductors* (Oxford University Press, New York, 1997), p. 43.